DOI: 10.36253/ijam-3982

REFERENCE EVAPOTRANSPIRATION ESTIMATION WITH NEURAL NETWORKS AND ERA5 REANALYSIS IN DATA-SPARSE REGIONS

Eduardo Morgan Uliana[1*], Uilson Ricardo Venâncio Aires[2], Marionei Fomaca de Sousa Junior[3], Demetrius David da Silva[4], Marcelo Ribeiro Viola[5], Ricardo Santos Silva Amorim[6], Kelte Resende Arantes[7], Marcio Roggia Zanuzo[8], Herval Alves Ramos Filho[9], Matheus Picalho Leal[10]

1* Instituto de Ciências Agrárias e Ambientais (ICAA), Universidade Federal de Mato Grosso, Sinop, 78550-728, Brazil. ORCID: https://orcid.org/0000-0003-2107-4634, eduardo.uliana@ufmt.br (corresponding author)

2*Department of Agricultural and Biological Engineering, Mississippi State University, Starkville, 39759, United States. ORCID: https://orcid.org/0000-0002-6745-2787, uilson.aires@msstate.edu

3 Department of Agricultural and Biological Engineering, Mississippi State University, Starkville, 39759, United States. ORCID: http://orcid.org/0000-0003-2048-6506, mf1521@msstate.edu

4Departamento de Engenharia Agrícola, Universidade Federal de Viçosa, Viçosa, 36570-000, Brazil. ORCID: https://orcid.org/0000-0001-9666-7421, demetrius@ufv.br

5 Departamento de Engenharia de Água e Solo, Universidade Federal de Lavras, Lavras, 37200000, Brasil. ORCID: https://orcid.org/0000-0002-3910-0987, marcelo.viola@ufla.br

6Departamento de Engenharia Agrícola, Universidade Federal de Viçosa, Viçosa, 36570-000, Brazil. ORCID: https://orcid.org/0000-0002-4570-1770, rsamorim@ufv.br

7Instituto de Ciências Agrárias e Ambientais (ICAA), Universidade Federal de Mato Grosso, Sinop, 78550-728, Brazil. ORCID: https://orcid.org/0000-0003-4007-4744, keltearantes@gmail.com

8Instituto de Ciências Agrárias e Ambientais (ICAA), Universidade Federal de Mato Grosso, Sinop, 78550-728, Brazil. ORCID: https://orcid.org/0000-0002-2957-2198, marcio.zanuzo@ufmt.br

9 Programa de Pós-Graduação em Recursos Hídricos, Universidade Federal de Mato Grosso, Cuiabá, 78060900, Brazil. ORCID: https://orcid.org/0009-0006-4137-8677, hervalarfilho@gmail.com

10 Instituto de Ciências Agrárias e Ambientais (ICAA), Universidade Federal de Mato Grosso, Sinop, 78550-728, Brazil. ORCID: https://orcid.org/0009-0007-1106-6792, e-mail: leall.ma@outlook.com

Abstract

Reference evapotranspiration (ET_0) is a fundamental hydrological variable for quantifying crop water requirements, conducting watershed water balance assessments, and optimizing irrigation management. However, the limited availability of high-quality meteorological data hinders the accurate determination of ET_0 across most regions of Brazil. Therefore, this study aimed to estimate ET0 in areas lacking meteorological observations by employing ERA5 reanalysis climate data and artificial neural network (ANN) models, as well as to evaluate its spatial and temporal variability. Observational data from 32 automated weather stations in the State of Mato Grosso, Brazil, were utilized to estimate ET_0 using the Penman-Monteith FAO56 method. These estimates were linked to ERA5 meteorological data, including global solar radiation and top-of-atmosphere radiation, using ANN models. The Mann-Kendall test was applied to detect trends in the ET_0 time series for the period 1980–2019. In Mato Grosso, the Pantanal biome exhibited the highest ET_0 values from October to March, followed by the Cerrado (Brazilian Savanna) and Amazon biomes. Statewide, the peak evapotranspirative demand occurred in August, September, and October, whereas April, May, and June recorded the lowest values. All biomes in Mato Grosso contained areas with statistically significant increasing trends in ET_0. The proposed models demonstrated satisfactory error metrics for ET_0 estimation, and the methodological approach enabled a robust assessment of the spatiotemporal dynamics of this hydrological variable, facilitating ET_0 estimation even in data-scarce regions.

Keywords: Pantanal, Amazon, trend analysis, Penman-Monteith FAO56, agricultural meteorology.

Highlights

• ERA5 reanalysis data and ANNs enable ET_0 estimation in data-scarce regions.

• Pantanal shows highest ET_0 values Oct-Mar, Amazon most affected by trends.

• ANN models achieved 5- 8% MAE for monthly ET_0 estimation across biomes.

• Increasing ET_0 trends detected 1980-2019 in all Mato Grosso biomes.

• Top-of-atmosphere radiation replaces surface data for regional ET_0 mapping.

1. Introduction

Evapotranspiration is a critical component of the hydrological cycle, representing the phase transition of water from liquid to vapor and encompassing both vegetation transpiration via stomatal regulation and evaporation from soil and open water surfaces. In tropical and subtropical regions, evapotranspiration constitutes the principal pathway for water loss to the atmosphere (Saha *et al*., 2022; Tari *et al*., 2022; Xiong *et al*., 2022; Walls *et al*., 2020). According to Dai *et al*. (2022) and Tian *et al*. (2018), it is a key meteorological variable governing the exchange of heat and moisture within the soil-plant-atmosphere continuum. Accurate determination of evapotranspiration is essential for quantifying crop water balance, designing irrigation systems, managing water resources, and conducting hydrological modeling at the watershed scale (Gocić & Arab Amiri, 2021; Liu *et al*., 2017; Walls *et al*., 2020; Woldesenbet & Elagib, 2021).

According to Silva *et al*. (2022), utilizing United Nations projections, the global population is expected to reach 9.7 billion by 2050, resulting in increased food demand and, consequently, greater agricultural water consumption, which currently accounts for approximately 70% of global freshwater withdrawals. Accurate determination of reference evapotranspiration (ET_0) is essential for optimizing agricultural water use efficiency and mitigating the impact of rising water demand. ET_0 underpins the estimation of crop evapotranspiration (ETc) at the field scale, following the methodology outlined by Allen *et al.* (1998), in which ET_0 is multiplied by the crop coefficient (Kc). Given its importance, this research focuses on determining ET_0 for Mato Grosso State, a leading region in national grain production.

Allen et al. (1998) define ET_0 as the evapotranspiration from a hypothetical reference surface consisting of a well-watered grass of uniform height (12 cm), with a fixed surface resistance to vapor transport of 70 s m^{-1}, an albedo of 0.23, and no limitations due to water stress, nutrient deficiencies, or pests. Direct measurement of ET_0 can be accomplished using a weighing lysimeter; however, this instrument is technically complex and incurs substantial costs for acquisition, maintenance, and operation (ranging from $5,000 to $30,000 USD), which restricts its widespread application at a large scale in Mato Grosso (Walls *et al*., 2020; Saha *et al*., 2022).

Beyond lysimeter measurements, indirect approaches for estimating evapotranspiration using meteorological data have been developed. The most accurate estimates are achieved with atmospheric profile methods, which necessitate detailed surface energy balance components and vertical gradients of temperature and vapor pressure above the plant canopy. Acquisition of these gradients requires installing micrometeorological towers equipped with sensors at multiple heights.

A prominent example of an atmospheric profile method is the Bowen Ratio-Energy Balance (BREB) technique. As with lysimeter-based approaches, Walls *et al*. (2020) report that the substantial costs associated with instrumentation have significantly limited the implementation of atmospheric profile methods. Yan et al. (2022) and Liu et al. (2012) corroborate this, noting that conventional techniques rely on expensive ground-based stations that yield only point-scale measurements, thereby constraining their spatial representativeness and utility for regional-scale analyses.

To address the limitations of profile methods, aerodynamic approaches have been integrated with the Bowen ratio, thereby reducing the need for extensive monitoring tower installations and improving the operational feasibility of evapotranspiration estimation. This classical methodology transforms two-level profile techniques into a more practical approach, requiring meteorological measurements at only a single height above the reference surface (Pereira, Sediyama, & Villa Nova, 2013). As a result, the Penman method was developed and subsequently parameterized, culminating in the Penman-Monteith FAO56 equation (Allen et al., 1998). The Penman-Monteith FAO56 equation is a physically based model that integrates thermodynamic and aerodynamic principles and enables the estimation of ET_0 using the following routine surface meteorological variables: (1) global solar radiation or sunshine duration, (2) maximum air temperature, (3) minimum air temperature, (4) relative humidity, and (5) wind speed (Nouri & Homaee, 2022).

The World Meteorological Organization (WMO) and the Food and Agriculture Organization of the United Nations (FAO) recommend the Penman-Monteith FAO56 (PM-FAO56) method as the standard protocol for estimating reference evapotranspiration (ET_0), owing to its extensive validation across diverse agroclimatic conditions worldwide (Woldesenbet & Elagib, 2021; Laqui *et al*., 2019; Rodrigues & Braga, 2021; Dai *et al*., 2022). As noted by Rodrigues and Braga (2021), the PM-FAO56 method is regarded as a robust and universally applicable ET_0 estimator, eliminating the necessity for region-specific parameter calibration. Empirical studies conducted in Brazil by Barros *et al.* (2009) and Santiago *et al.* (2002) compared lysimetric measurements with Penman-Monteith FAO56 estimates, demonstrating the method's superior accuracy relative to observed data.

Despite the operational simplicity and scalability of the PM-FAO56 method, which requires only surface meteorological variables, significant limitations persist in regions with sparse meteorological monitoring infrastructure, such as Brazil. For instance, the State of Mato Grosso, situated in the Central-West region of Brazil, encompasses approximately 903,000 km² but is served by only 34 automatic weather stations within the official network of the National Institute of Meteorology (INMET). This limited spatial distribution of meteorological data presents substantial challenges for accurately estimating reference evapotranspiration (ET_0) using the PM-FAO56 method across most of the state, which is recognized as a national leader in agricultural production. As highlighted by Nouri and Homaee (2022), data scarcity poses a critical impediment to agricultural and hydrological planning, necessitating alternative methodologies to address these informational gaps.

Within this framework, integrating climate reanalysis datasets with artificial intelligence (AI) methodologies represents a promising approach for quantifying the spatial and temporal variability of reference evapotranspiration (ET_0) in regions lacking meteorological station coverage. As demonstrated by Abrishami et al. (2019), artificial neural networks (ANNs) exhibit a high degree of proficiency in parameter estimation and in modeling the complex, nonlinear interactions between meteorological variables and ET_0. Laqui *et al*. (2019) emphasized that ANN-based models constitute a viable solution for ET_0 estimation under data-limited conditions. Several studies, including those by Elbeltagi *et al*. (2022), Abrishami, Sepaskhah, and Shahrokhnia (2019), Walls *et al*. (2020), and Gocić & Arab Amiri (2021), have assessed the applicability of ANNs for evapotranspiration estimation, consistently concluding that these AI models provide robust performance for this hydrometeorological variable. Nonetheless, most ET_0 estimations employing ANNs have relied on surface meteorological inputs, the availability of which remains limited in many developing regions. Consequently, there is a pressing need to utilize alternative data sources, such as climate reanalyses, to enhance ET_0 estimation capabilities. These datasets offer significant potential to advance environmental research, optimize agricultural management, inform urban planning, and guide public policy development in areas characterized by sparse meteorological monitoring networks.

Climate reanalysis products integrate previous short-term numerical weather forecasts with surface-based observational datasets, providing a physically consistent and spatially continuous source of atmospheric parameters for characterizing weather and climate. Due to their gridded structure, reanalysis datasets enable the estimation of reference evapotranspiration (ET_0) in areas with limited meteorological observations, while also facilitating comprehensive analyses of its spatial and temporal variability. Rodrigues and Braga (2021) employed NASA POWER reanalysis data to estimate ET_0 and reported a high degree of concordance between observed ET_0 values and those derived from the reanalysis dataset.

Nouri and Homaee (2022) assessed the performance of reference evapotranspiration (ET_0) estimates derived from climate reanalysis products, concluding that ERA5 yielded more accurate daily and monthly ET_0 values compared to GLDAS2 and MERRA2 for 84% of analyzed sites in Iran. The authors identified ERA5 reanalysis meteorological data, at both daily and monthly temporal resolutions, as a superior alternative for estimating ET_0 in hydrological and crop modeling applications, as well as for irrigation management in regions with limited observational data. Their literature-based synthesis further substantiated the enhanced quality of ERA5 relative to other reanalysis datasets. Nonetheless, ERA5 has yet to be systematically applied for ET_0 estimation within the study region addressed in this research, highlighting the need to extend its utilization to additional geographic contexts.

Given the critical role of reference evapotranspiration (ET_0) in the design and management of irrigation systems and in watershed water balance assessments, the objective of this study was to estimate ET_0 using ERA5 reanalysis climate data and artificial neural network (ANN) models for locations in the State of Mato Grosso characterized by insufficient meteorological monitoring. Furthermore, this research aimed to evaluate the spatial and temporal variability of ET_0 across these data-scarce regions.

2. Methods

2.1. Study Area

The study area comprised the State of Mato Grosso (Figure 1), situated in the Central-West region of Brazil, which is internationally recognized for its substantial agricultural output of soybean (*Glycine max* L.), maize (*Zea mays* L.), common bean (*Phaseolus vulgaris* L.), and cotton (*Gossypium* spp.). The respective crop yields were estimated at 29,778.5, 28,555.9, 305.2, and 2,397.9 thousand metric tons, based on the 2017 Agricultural Census (IBGE, 2017). The cultivated area for each crop was approximately 8,862.7, 4,829.7, 207.0, and 596.6 thousand hectares, respectively.

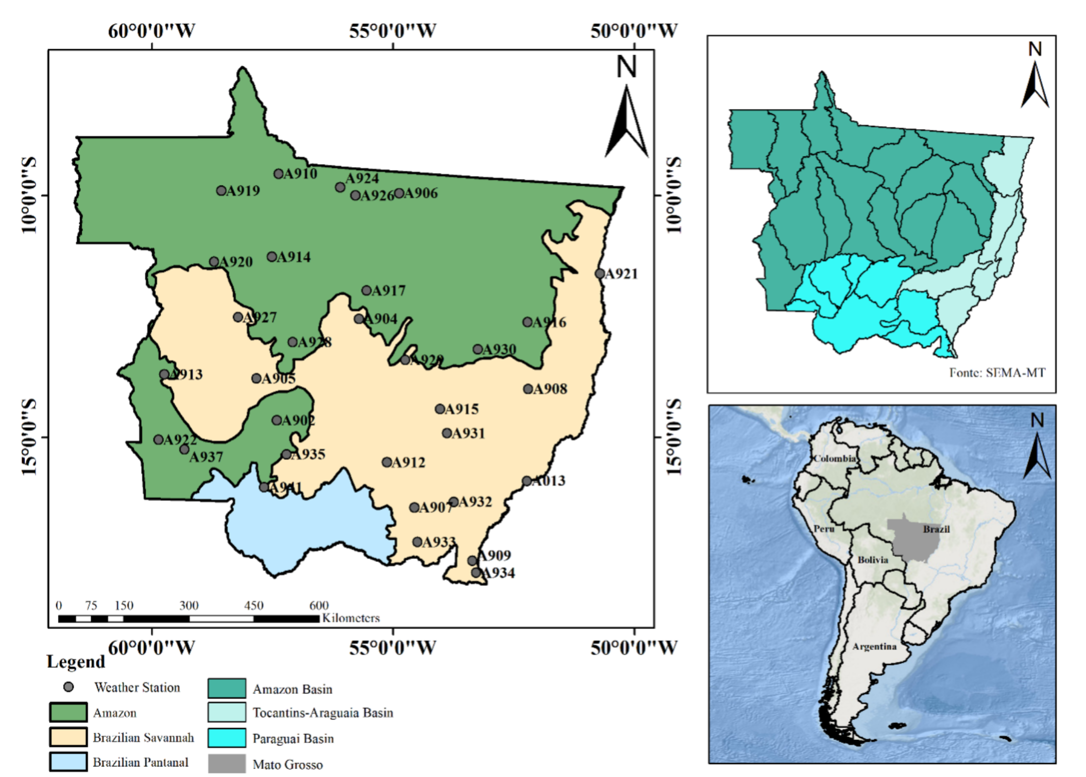

Figure 1. Map of the State of Mato Grosso highlighting the location of automatic meteorological stations, biomes, and main river basins within its territory.

As noted by Carvalho *et al*. (2022), the primary agricultural region of Mato Grosso experiences a distinct seasonality, with the wet season occurring from October to April and the dry season from May to September. Soybean (*Glycine max* L.) and maize (*Zea mays* L.), which represent the principal crops in the state, are typically sown during the austral spring and summer, coinciding with the rainy season. However, there is an increasing adoption of supplemental irrigation techniques for third-crop production, as well as to mitigate the effects of water deficits on soybean and maize during periods of reduced precipitation. Common bean (*Phaseolus vulgaris* L.) is predominantly cultivated during the winter (third crop), a period characterized by minimal monthly precipitation, necessitating full irrigation to sustain crop growth.

According to the National Water and Sanitation Agency (ANA, 2019, 2020), the state of Mato Grosso has exhibited significant expansion in irrigated agriculture, resulting in the establishment of irrigation districts within the Alto Rio das Mortes and Alto Teles Pires river basins. This development has enhanced the region's relevance in the national context and fostered the advancement of croplands managed by center pivot irrigation systems. In both the short-term (2010-2017) and medium-term (2000-2017), Mato Grosso led the country in irrigation growth rates and demonstrated substantial potential for further expansion of irrigated areas. Moreover, the adoption of center pivot irrigation technologies in Mato Grosso has consistently increased, serving to mitigate the impacts of intra-seasonal droughts during the wet season and to sustain optimal crop development throughout the dry season (May to September).

In addition to its substantial agricultural output, the state of Mato Grosso is distinguished by the presence of three major Brazilian biomes: the Pantanal, the *Cerrado* (Brazilian Savanna), and the Amazon. The region includes the headwaters of three principal river basins essential for national hydrological security: the Tocantins-Araguaia, the Amazon (including the upper Tapajós and Xingu Rivers), and the Paraguay River (Figure 1).

Therefore, Mato Grosso was selected as the focus of this research due to its substantial relevance to Brazilian agricultural production, necessitating highly accurate evapotranspiration data, which is essential for the engineering and operational management of advanced irrigation systems. The state exhibits diverse cropping calendars and heterogeneous water requirements, presenting a significant challenge for hydrological resource management and the development of sustainable agricultural practices. This scenario underscores the need for comprehensive analysis of hydrometeorological processes, particularly evapotranspiration. Furthermore, the environmental complexity of Mato Grosso, with its inclusion of three biomes exhibiting distinct climatic, edaphic, and ecological characteristics, renders it an optimal setting for evaluating the performance of evapotranspiration estimation models under varied agro-environmental conditions.

2.2. Meteorological Data

For the estimation of reference evapotranspiration in Mato Grosso, meteorological observations from 32 automatic weather stations (Table 1; Figure 1) operated by the National Institute of Meteorology (INMET) were utilized. Hourly measurements of key meteorological variables, including maximum air temperature (°C), minimum air temperature (°C), dew point temperature (°C), maximum relative humidity (%), minimum relative humidity (%), global solar radiation (MJ m^{-2} day^{-1}), and wind speed (m s^{-1}), were processed to obtain daily mean values and cumulative totals.

Table 1. Automatic weather stations in the State of Mato Grosso employed in this study, operated by the National Institute of Meteorology (INMET)

Code	Municipality	Biome	Latitude	Longitude	Altitude (m)	Time Period
A924	Alta Floresta	Amazônia	09°50'S	56°06'W	289	2008-2020
A910	Apiacás	Amazônia	09°33'S	57°23'W	220	2007-2020
A926	Carlinda	Amazônia	10°00'S	55°47'W	290	2008-2020
A913	Comodoro	Amazônia	13°42'S	59°45'W	591	2007-2020
A919	Cotriguaçu	Amazônia	09°54'S	58°34'W	261	2007-2020
A930	Gaúcha do Norte	Amazônia	13°11'S	53°15'W	379	2009-2020
A906	Guarantã do Norte	Amazônia	09°57'S	54°53'W	320	2003-2020
A914	Juara	Amazônia	11°16'S	57°31'W	260	2007-2020
A920	Juína	Amazônia	11°22'S	58°43'W	200	2008-2020
A928	Nova Maringá	Amazônia	13°02'S	57°05'W	353	2007-2020
A937	Pontes e Lacerda	Amazônia	15°15'S	59°20'W	256	2008-2020
A916	Querência	Amazônia	12°37'S	52°13'W	382	2007-2020
A917	Sinop	Amazônia	11°58'S	55°33'W	371	2007-2020
A902	Tangará da Serra	Amazônia	14°39'S	57°25'W	322	2003-2020
A922	Vila Bela da Santissíma Trindade	Amazônia	15°03'S	59°52'W	222	2007-2020
A908	Água Boa	Brazilian Savannah	14°00'S	52°12'W	432	2007-2020
A909	Alto Araguaia	Brazilian Savannah	17°33'S	53°22'W	753	2012-2020
A934	Alto Taquari	Brazilian Savannah	17°48'S	53°17'W	875	2008-2020
A013	Aragarças	Brazilian Savannah	15°54'S	52°14'W	347	2007-2020
A927	Mundo Novo	Brazilian Savannah	12°31'S	58°13'W	431	2008-2020
A905	Campo Novo do Parecis	Brazilian Savannah	13°47'S	57°50'W	570	2003-2020
A912	Campo Verde	Brazilian Savannah	15°31'S	55°08'W	749	2007-2020
A932	Guiratinga	Brazilian Savannah	16°20'S	53°45'W	526	2008-2020
A933	Itiquira	Brazilian Savannah	17°10'S	54°30'W	585	2009-2020
A929	Nova Ubiratã	Brazilian Savannah	13°24'S	54°45'W	518	2008-2020
A915	Paranatinga	Brazilian Savannah	14°25'S	54°02'W	474	2007-2020
A935	Porto Estrela	Brazilian Savannah	15°21'S	57°13'W	145	2008-2020
A907	Rondonópolis	Brazilian Savannah	16°27'S	54°34'W	284	2004-2020
A931	Santo Antônio do Leste	Brazilian Savannah	14°55'S	53°53'W	648	2008-2020
A921	São Félix do Araguaia	Brazilian Savannah	11°37'S	50°43'W	218	2009-2020
A904	Sorriso	Brazilian Savannah	12°33'S	55°43'W	380	2003-2020
A941	Cáceres	Pantanal	16°02'S	57°41'W	116	2012-2020

2.3. Reference Evapotranspiration Estimation (ET_0 - FAO56)

Reference evapotranspiration (ET_0) was calculated according to the Penman-Monteith FAO-56 methodology (Allen et al., 1998), a standard procedure in agrometeorological studies, as represented by the following equation:

$$ET_0=\frac{0.408\Delta(Rn\text{-}G)+\gamma\frac{900}{T+273}U_2(e_s\text{-}e_a)}{\Delta+\gamma(1+0.34U_2)} \quad (1)$$

where: ET_0 is the reference evapotranspiration (mm d^{-1}); Rn is the net radiation (MJ m^{-2}); G is the soil heat flux density (MJ m^{-2}); T is the mean air temperature (ºC); U_2 is the wind speed at 2 meters height (m s^{-1}); e_s is the saturation vapor pressure (kPa); e_a is the actual vapor pressure (kPa); Δ is the slope of the vapor pressure curve at temperature T (kPa $ºC^{-1}$); γ is the psychrometric constant (kPa $ºC^{-1}$). The estimation of reference evapotranspiration and the parameterization of the variables in Equation 1, in accordance with the FAO 56 guidelines (Allen *et al*., 1998), were conducted using the "Evapotranspiration" package in the R statistical software (R Core Team, 2021), as developed by Guo, Westra, and Peterson (2022). The computational routine utilized daily meteorological variables measured at the stations listed in Table 1, including maximum air temperature (°C), minimum air temperature (°C), maximum relative humidity (%), minimum relative humidity (%), global solar radiation (MJ m^{-2} day^{-1}), and wind speed (m s^{-1}).
Following the calculation of daily reference evapotranspiration (ET_0) for the periods specified in Table 1, the monthly mean daily ET_0 (mm day^{-1}), total monthly ET_0 (mm $month^{-1}$), and monthly maximum daily ET_0 values (mm day^{-1}) were derived. Further details regarding the parameterizations and equations applied can be found in the article and supplementary materials by Guo et al. (2016).

2.4. ERA5 Reanalysis Data

Daily ERA5 reanalysis data (Copernicus Climate Change Service, 2017) covering the period from January 1, 1980, to December 31, 2019, were acquired from the ECMWF/ERA5/DAILY dataset via the Google Earth Engine (GEE) platform (Gorelick *et al*., 2017), a cloud-based system designed for large-scale geospatial analysis. The methodology for accessing ERA5 reanalysis data was consistent with the approach described by Uliana et al. (2024).
ERA5 is the fifth-generation global atmospheric reanalysis produced by the European Centre for Medium-Range Weather Forecasts (ECMWF), integrating numerical model outputs with assimilated observational data from diverse global sources (Hersbach et al., 2020). The dataset provides daily aggregated values for

nine meteorological variables, as detailed in Table 2, on a spatial grid with an approximate resolution of 28 km. Hourly ERA5 outputs were processed to obtain daily aggregated values for each parameter. In this study, only variables exhibiting a direct physical association with reference evapotranspiration (ET_0) were selected as input parameters for the artificial neural network models. Consequently, "Total Precipitation" and "Mean Sea Level Pressure" were omitted from the dataset and excluded from all subsequent analyses.

Table 2. Details of the ERA5 reanalysis data bands available on a daily scale in the Google Earth Engine library.

Description	Unit	Bands[1]
Average air temperature at 2m height	Kelvin	mean_2m_air_temperature
Minimum air temperature at 2m height	Kelvin	minimum_2m_air_temperature
Maximum air temperature at 2m height	Kelvin	maximum_2m_air_temperature
Dewpoint temperature at 2m height	Kelvin	dewpoint_2m_temperature
Total precipitation	m	total_precipitation
Surface pressure	Pa	surface_pressure
Mean sea level pressure	Pa	mean_sea_level_pressure
10m u-component of wind (u)	$m\ s^{-1}$	u_component_of_wind_10m
10m v-component of wind (v)	$m\ s^{-1}$	v_component_of_wind_10m

[1] Band code available in the "ECMWF/ERA5/DAILY" collection on Google Earth Engine.

All available daily satellite images of the meteorological variables specified in Table 2, with the exception of total precipitation and mean sea-level pressure, were retrieved in GeoTIFF format via Google Earth Engine. The data for each variable were subsequently extracted on a pixel-by-pixel basis, temporally organized, and stored as time series vectors using a MATLAB-based computational routine.

The scalar wind speed (V, in $m\ s^{-1}$) was computed using the equation: $V=\sqrt{u^2+v^2}$, where u and v represent the zonal and meridional wind components, respectively. Temperature and surface pressure measurements were converted to degrees Celsius (°C) and hectopascals (hPa). For each grid cell, historical time series of mean monthly air temperature, dewpoint temperature, surface pressure, and wind speed were generated. The ERA5 reanalysis dataset (1980–2019) was referenced and systematically organized for the study region according to the methodologies described in this section.

2.5. ANN Architecture and Training

ANN models were developed to relate the monthly ERA5 data from the 32 meteorological stations with the respective values of monthly average ET_0, total monthly ET_0, and maximum daily ET_0 determined using the Penman-Monteith-FAO56 method (Allen *et al*., 1998). Monthly ERA5 data for maximum temperature, minimum temperature, mean temperature, dew point temperature, surface pressure, and wind speed were used as input data for the ANNs. The procedures employed in this study for selecting input data, preprocessing these data, and training the Artificial Neural Networks (ANNs) were similar to those used by Uliana et al. (2024) in estimating lake evaporation using ERA5 reanalysis data and ANNs.

In addition to the ERA5 meteorological variables, top-of-atmosphere solar radiation - R_0 (monthly total) and estimated global solar radiation - R_S (monthly mean) were incorporated as input parameters. Top-of-atmosphere solar radiation was computed for each grid cell based on the day of the year and latitude. Monthly mean global solar radiation values were derived from the spatial grid presented by Morgan et al. (2025), which was developed using the same ERA5 reanalysis dataset employed in the present study and subsequently calibrated with surface observations from meteorological stations. Both radiation variables were incorporated into the analysis to quantify their contributions to the predictive performance of the Artificial Neural Network models.

The eight input variables were selected as they represent the principal physical determinants of reference evapotranspiration (ET_0) as defined by the FAO-56 Penman–Monteith methodology. As detailed by Allen et al. (1998), maximum, minimum, and mean air temperatures delineate the thermal regime and influence the calculation of saturation vapor pressure, the slope of the saturation vapor pressure curve, and longwave radiation flux. Dew point temperature provides essential quantification of actual vapor pressure and atmospheric vapor pressure deficit, while wind speed governs the aerodynamic transfer of sensible heat and water vapor. Surface atmospheric pressure establishes the psychrometric constant, thereby accounting for atmospheric effects related to site elevation. Extraterrestrial solar radiation denotes the astronomical component of incident solar energy, whereas global solar radiation measures the actual shortwave energy reaching the terrestrial surface. Collectively, these variables encompass the thermal, aerodynamic, hygrometric, and radiative components fundamental to the estimation of reference evapotranspiration.

Therefore, the developed model utilized eight meteorological input variables and produced a single output variable, representing reference evapotranspiration (ET_0). It is noteworthy that the input dataset was consistent across the three network architectures, with variation occurring solely in the output variables, which comprised the monthly mean daily ET_0 ($\overline{ET}_0$), total monthly ET_0 ($\overline{ET}_{0\text{ - Total}}$), and maximum daily ET_0 ($\overline{ET}_{0\text{ - Max}}$) for each month, in accordance with the specific objectives of each analysis.

In addition to the computational simplicity of determining extraterrestrial radiation (R0) and incorporating latitude and day of the year in its estimation, these parameters were indirectly integrated into the artificial neural network (ANN) models. This approach enhanced both the accuracy and precision of ET_0 regionalization.

For model calibration, input variables corresponding to each period of the year and ANN outputs were normalized according to Equation 2. Following normalization, the dataset was randomly partitioned into three subsets: training (60%), validation (30%), and test (10%) samples. The normalization methodology (Equation 2) was similarly employed by Ramos Filho et al. (2024) and Sousa Jr. et al. (2024) in their applications of artificial neural networks (ANNs) for environmental modeling.

$$pn = \frac{2(p\text{-}minp)}{(maxp\text{-}minp)} - 1 \tag{2}$$

where: pn is the normalized value (ranging between -1 and 1), p is the value of the variable, minp and maxp are the minimum and maximum values of the variable in the series under study, respectively.

The multilayer perceptron (MLP) (Figure 2) was adopted as the neural network framework. The artificial neural networks (ANNs) were configured with a single input layer, two hidden layers, and one output layer. Within the hidden layers, log-sigmoid (logsig) and hyperbolic tangent sigmoid (tansig) activation functions were assessed, while a linear activation function was implemented in the output layer of the ANNs.

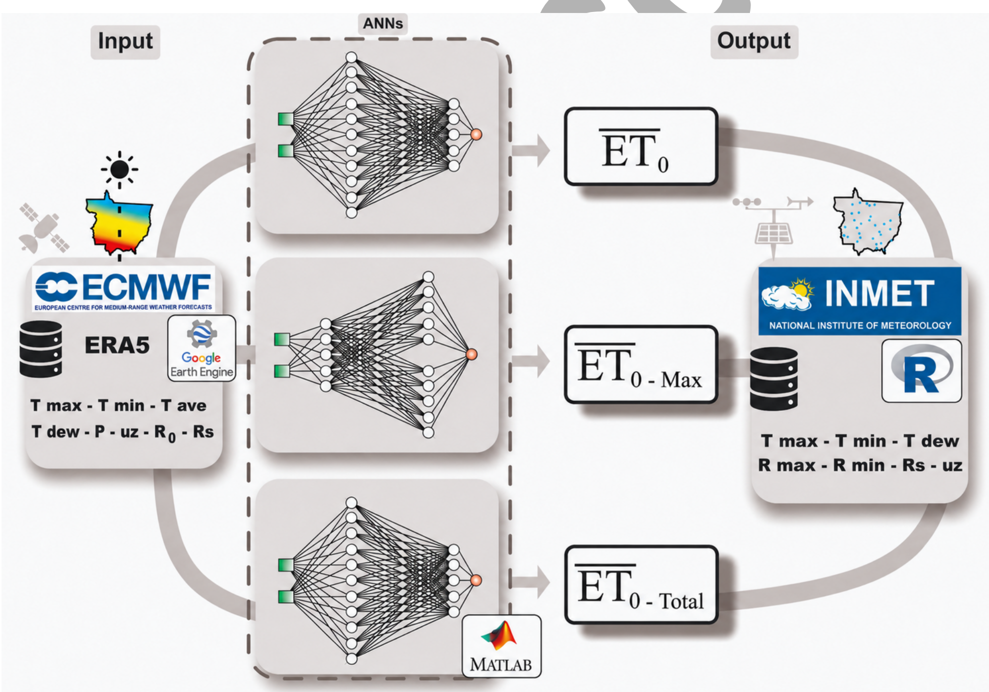

Figure 2. Representation of a multilayer perceptron ANN architecture.

The MLP architecture was chosen over more complex models, such as long short-term memory (LSTM) networks or one-dimensional convolutional neural networks (1D-CNNs), due to the relatively limited length of the available historical time series. These advanced architectures typically require more extensive datasets to effectively capture temporal dependencies or local sequential patterns and are more prone to overfitting when trained on restricted sample sizes. In this context, the MLP architecture offered a less complex structure, reduced computational cost, and sufficient capability to represent the nonlinear interactions between meteorological input variables and reference evapotranspiration (ET_0).

The quantity of artificial neurons in the hidden layers of the artificial neural networks (ANNs) was systematically optimized using the Shuffled Complex Evolution-University of Arizona (SCE-UA) algorithm (Duan et al., 1992) to minimize predictive errors in the estimation of reference evapotranspiration (ET_0). This optimization procedure was incorporated into the ANN training workflow, adopting the Kling-Gupta efficiency (KGE') index (Kling et al., 2012) as the performance criterion. To mitigate the risk of overfitting, the number of neurons in each hidden layer was limited to a maximum of 15. Furthermore, the Levenberg-Marquardt algorithm was employed to enhance the convergence and stability of the ANN training process.

2.6. Evaluation of ANN Performance

To assess the performance of the artificial neural networks (ANNs) in estimating reference evapotranspiration (ET_0), the following statistical indicators were employed: mean absolute error (MAE, Equation 3), root mean square error (RMSE, Equation 4), bias (Equation 5), Nash–Sutcliffe efficiency coefficient (NSE, Equation 6), Kling-Gupta efficiency coefficient (KGE, Equation 7), and a paired t-test at the 5% significance level (Equation 8). These statistical metrics are commonly adopted in agrometeorological modeling studies and were also utilized by Uliana et al. (2024) for ANN performance evaluation Further interpretation details are available in the cited study.

$$\mathrm{MAE}=\frac{1}{\mathrm{N}}\sum_{\mathrm{i}=1}^{\mathrm{N}}|\mathrm{O_i}-\mathrm{P_i}| \tag{3}$$

$$\mathrm{RMSE}=\left[\frac{1}{\mathrm{N}}\sum_{\mathrm{i}=1}^{\mathrm{N}}(\mathrm{O_i}-\mathrm{P_i})^2\right]^{0,5} \tag{4}$$

$$\text{bias}=\frac{1}{N}\sum_{i=1}^{N}(O_i-P_i) \tag{5}$$

$$E_{NS} = 1-\frac{\sum_{i=1}^{n}(O_i-P_i)^2}{\sum_{i=1}^{n}(O_i-O)^2} \tag{6}$$

$$E_{kg}=1-\sqrt{(r-1)^2+\left(\frac{\sigma_e}{\sigma_o}-1\right)^2+(\text{bias}-1)^2} \tag{7}$$

$$t=\sqrt{\left[\frac{(n-1)\ \text{bias}^2}{\text{RMSE}^2-\text{bias}^2}\right]} \tag{8}$$

where P_i is the estimated evapotranspiration (mm), O_i is the observed evapotranspiration (mm), O is the mean of the observed evapotranspiration (mm), n is the number of sample values, r is the correlation coefficient between the observed and estimated data, σ_e is the standard deviation of the data estimated using the model, and σ_o is the standard deviation of the observed data.

The statistical indicators were computed separately for the training, validation, and testing phases of the artificial neural networks (ANNs). This strategy enabled the assessment of both model calibration, using the dataset employed for network training, and the model's generalization capacity when tested on independent data. Additionally, leave-one-out cross-validation (LOOCV) was implemented as a supplementary evaluation protocol. In this method, the data from each meteorological station were sequentially excluded from the modeling dataset and subsequently utilized for model testing, with the neural network trained on data from the remaining stations. Model performance under LOOCV was evaluated using the same statistical indicators as those applied during the training, validation, and testing phases. This methodology provided a more robust evaluation of the predictive capability and generalization potential of the ANNs in agrometeorological applications.

Based on the best ANN model selected using the presented metrics, the estimation of $\overline{ET}_0$, $\overline{ET}_{0\text{ - Total}}$ and $\overline{ET}_{0\text{ - Max}}$ was performed for the period from January 1980 to December 2019 for all reanalysis grid pixels. Following this procedure, the Mann–Kendall test was conducted at a 5% significance level to assess the presence of statistically significant trends in the historical reference evapotranspiration ($\overline{ET}_0$) time series. For grid cells exhibiting significant trends, the magnitude of change was quantified using the Theil–Sen slope estimator, which was calculated as the median of all slopes derived from pairwise comparisons of observations. The slope was initially estimated on a monthly timescale and subsequently converted to a decadal rate by multiplying the monthly value by 120. Consequently, the rates of change were expressed in millimeters per day per decade (mm day^{-1} $decade^{-1}$), where positive values denote an increasing trend and negative values denote a decreasing trend in ET_0 throughout the analyzed period.

3. Results

Figure 3 shows the average monthly values of the meteorological variables measured at INMET automatic stations located in the Amazon, Brazilian Savannah, and Pantanal biomes (Table 1). From September to April, the Pantanal region records the highest values of maximum temperature (Tmax). However, between May and September, the maximum temperature in the Amazon exceeded that observed in the other biomes.

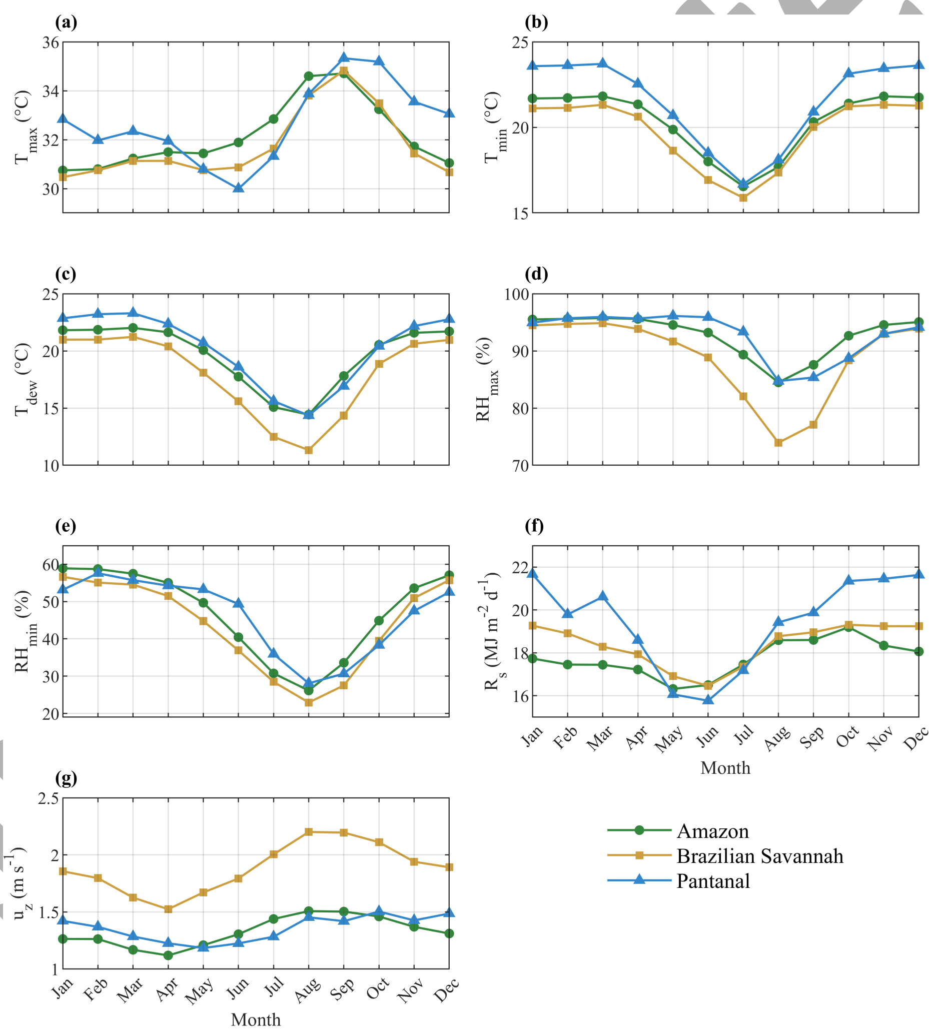

Figure 3. Average monthly values for the three biomes in the State of Mato Grosso of the meteorological variables recorded at the INMET automatic stations used to estimate reference evapotranspiration (ET_0) with the Penman-Monteith-FAO56 method.

The highest minimum temperature (Tmin) values were recorded in the Pantanal region, whereas the lowest values were found in the Brazilian Savannah region. The minimum temperature in the Amazon was closer to that observed in the Brazilian Savannah, although slightly higher. The lowest dew point temperature (Tdew) values occurred in the Brazilian Savannah throughout the year, and this biome also showed the lowest values of maximum (Rmax) and minimum (Rmin) relative humidity. Between June and September, there was a discernible variation in the maximum relative humidity, which might have led to higher evapotranspiration.

Regarding global solar radiation (Rs), Figure 3 shows that the Pantanal exhibited the highest values between August and April, while the lowest values occurred between May and July. Except for the behavior of solar radiation in winter and part of autumn in the Pantanal, the Amazon is the biome with the lowest average global solar radiation, compared to the other biomes, which may be associated with high cloud cover in the region. Finally, as shown in Figure 3, the Brazilian Savannah had the highest wind speed, a behavior that prevailed throughout the year. This analysis highlights the seasonality of meteorological elements related to the physical aspects of evapotranspiration in the different biomes of the State, providing a basis for understanding its spatial and temporal variability, which will be conducted next.

Table 3 presents the architecture of the Artificial Neural Networks (ANNs) used to estimate the average daily monthly reference evapotranspiration ($\overline{\mathrm{ET}}_0$), maximum daily monthly ($\overline{\mathrm{ET}}_{0\text{ - Max}}$), and total monthly ($\overline{\mathrm{ET}}_{0\text{ - Total}}$). In addition to the network architectures, the table reports the error metrics obtained during the training, validation, and testing phases, as well as those derived from leave-one-out cross-validation (LOOCV).

The MAE values presented in Table 3 correspond to approximately 5–8% of the average observed variable values. The RMSE values were 7%–9% of the average observed values. These values were within the acceptable range, and the models adequately estimated the variables. For both models, the bias was close to zero, which is desirable in a simulation. Positive values indicate that the models underestimated the variables of interest.

Table 3. Architecture of the Artificial Neural Networks (ANNs) and statistical error measures for estimating reference evapotranspiration in the State of Mato Grosso, using ERA5 reanalysis data and radiation as inputs.

Variable	Stage	Function	N_1	N_2	N_3	MAE	RMSE	BIAS	E_{NS}	E_{kg}	t
$\overline{ET}_0$	Training	tansig; logsig; purelin	7	5	1	0.2385	0.3141	-0.0030	0.7766	0.8307	0.3424$^{(ns)}$
	Validation					0.2611	0.3461	-0.0076	0.7111	0.8087	0.5508$^{(ns)}$
	Test					0.2499	0.3154	-0.0219	0.7312	0.8339	0.9999$^{(ns)}$
	LOOCV					0.2654	0.3576	-0.0028	0.7001	0.8009	0.3589$^{(ns)}$
$\overline{ET}_{0\text{ - Max}}$	Training	tansig; logsig; purelin	6	5	1	0.3641	0.4788	-0.0063	0.7440	0.8031	0.5161$^{(ns)}$
	Validation					0.3809	0.4901	0.0162	0.7102	0.7903	0.9162$^{(ns)}$
	Test					0.3671	0.4870	0.0325	0.7516	0.8054	1.0670$^{(ns)}$
	LOOCV					0.3824	0.5094	-0.0014	0.7058	0.7928	0.1408$^{(ns)}$
$\overline{ET}_{0\text{ - Total}}$	Training	tansig; logsig; purelin	5	5	1	7.2731	9.6372	-0.0592	0.7834	0.8354	0.2173$^{(ns)}$
	Validation					7.7162	10.0459	0.0539	0.7493	0.8215	0.1341$^{(ns)}$
	Test					7.2092	9.4237	-0.2360	0.7597	0.8595	0.3604$^{(ns)}$
	LOOCV					7.9027	10.7581	0.0023	0.7212	0.8081	0.0099$^{(ns)}$

$\overline{ET}_0$ is the average daily monthly evapotranspiration; $\overline{ET}_{0\text{ - Max}}$ is the maximum daily monthly evapotranspiration; $\overline{ET}_{0\text{ - Total}}$ is the total monthly evapotranspiration; LOOCV: leave-one-out cross-validation N_1, N_2 represent the number of artificial neurons in the two hidden layers; N_3 is the number of neurons in the output layer; logsig, tansig and purelin: log-sigmoid, hyperbolic tangent sigmoid, and linear transfer functions, respectively; MAE: mean absolute error (mm); RMSE: root mean square error (mm); BIAS: mm; E_{NS}: Nash-Sutcliffe efficiency index; E_{kg}: Kling-Gupta efficiency index; t: paired t-test statistic value; and ns: not significant at the 5% significance level.

The Nash-Sutcliffe Efficiency (E_{NS}) values obtained during the training, validation, testing, and leave-one-out cross-validation (LOOCV) phases indicated robust model performance in estimating reference evapotranspiration (ET_0), according to the classification proposed by Van Liew et al. (2007). The Kling-Gupta Efficiency (E_{kg}) values, ranging from 0.7903 to 0.8595, further confirmed strong concordance between observed and model-estimated ET_0 values generated by the artificial neural networks (ANNs). Additionally, results from the paired t-test indicated no statistically significant differences between observed and estimated ET_0 values at any evaluation stage, including LOOCV. Consequently, the null hypothesis of equality between observed and estimated values could not be rejected, supporting the reliability of the ANN-based modeling approach.

The results of the leave-one-out cross-validation (LOOCV) confirmed the generalization capability of the developed models. For mean reference evapotranspiration ($\overline{\mathrm{ET}}_0$), the LOOCV yielded mean absolute error (MAE) and root mean square error (RMSE) values of 0.2654 mm and 0.3576 mm, respectively, with a bias of -0.0028 mm, Nash-Sutcliffe Efficiency (NSE) of 0.7001, and Kling-Gupta Efficiency (KGE) of 0.8009. For maximum mean reference evapotranspiration ($\overline{\mathrm{ET}}_{0\text{ - Max}}$), the MAE was 0.3824 mm, RMSE was 0.5094 mm, bias was -0.0014 mm, NSE was 0.7058, and KGE was 0.7928. For total mean reference evapotranspiration ($\overline{\mathrm{ET}}_{0\text{ - Total}}$), the MAE was 7.9027 mm, RMSE was 10.7581 mm, bias was 0.0023 mm, NSE was 0.7212, and KGE was 0.8081.

The bias values obtained through leave-one-out cross-validation (LOOCV) remained close to zero for all three variables, indicating minimal systematic error. Moreover, the consistency between the performance metrics derived from LOOCV and those observed during the training, validation, and testing phases indicates that the predictive accuracy of the models remained robust when each individual observation was independently excluded from the calibration dataset.

With respect to the artificial neural network (ANN) architectures, although the maximum number of neurons permitted in each hidden layer was fixed at 15, the Shuffled Complex Evolution-University of Arizona (SCE-UA) optimization algorithm, using Kling–Gupta efficiency (KGE') index (Kling et al., 2012) as the objective function, identified optimal architectures containing between five and seven neurons per hidden layer. The resulting configurations were 7-5-1 for reference evapotranspiration ($\overline{\mathrm{ET}}_0$), 6-5-1 for maximum reference evapotranspiration ($\overline{\mathrm{ET}}_{0\text{ - Max}}$), and 5-5-1 for total reference evapotranspiration ($\overline{\mathrm{ET}}_{0\text{ - Total}}$).

The similarity among the error metrics obtained during the training, validation, testing, and leave-one-out cross-validation (LOOCV) phases indicates that the models demonstrated robust generalization capability, with no discernible evidence of overfitting. These findings underscore that the Shuffled Complex Evolution-University of Arizona (SCE-UA) algorithm constitutes a rigorous and effective method for optimizing the number of neurons in the hidden layers of artificial neural networks (ANNs) for reference evapotranspiration modeling.

During the training of the artificial neural networks, various combinations of the logarithmic sigmoid (logsig) and hyperbolic tangent sigmoid (tansig) activation functions were assessed. Employing identical activation functions in both hidden layers resulted in increased estimation errors. Accordingly, the optimal architectures utilized the tansig function in the first hidden layer and the logsig function in the second hidden layer. The linear activation function (purelin) was implemented in the output layer for all three ANN models. This configuration contributed to improved model accuracy and stability in reference evapotranspiration estimation.

Figure 4 illustrates the relationships between observed and model-estimated values generated by the artificial neural networks (ANNs) for monthly mean daily ($\overline{ET}_0$ – a,b,c), monthly maximum daily ($\overline{ET}_{0\text{ - Max}}$- d,e,f), and monthly total reference evapotranspiration ($\overline{ET}_{0\text{ - Total}}$- g,h,i) during the training, validation, and testing phases. Pearson's correlation coefficients (r) ranged from 0.8431 to 0.8851, while the coefficients of determination (R^2) ranged from 0.7109 to 0.7834, indicating a strong association between observed and estimated ET0 values. The proximity of the regression lines to the 1:1 reference lines further demonstrates strong agreement between observed and model-estimated ET_0 values.

Overall, the graphical analyses (figure 4) corroborate the statistical metrics presented in Table 3, demonstrating that the ANN models achieved satisfactory precision, accuracy, and generalization capability in estimating reference evapotranspiration.

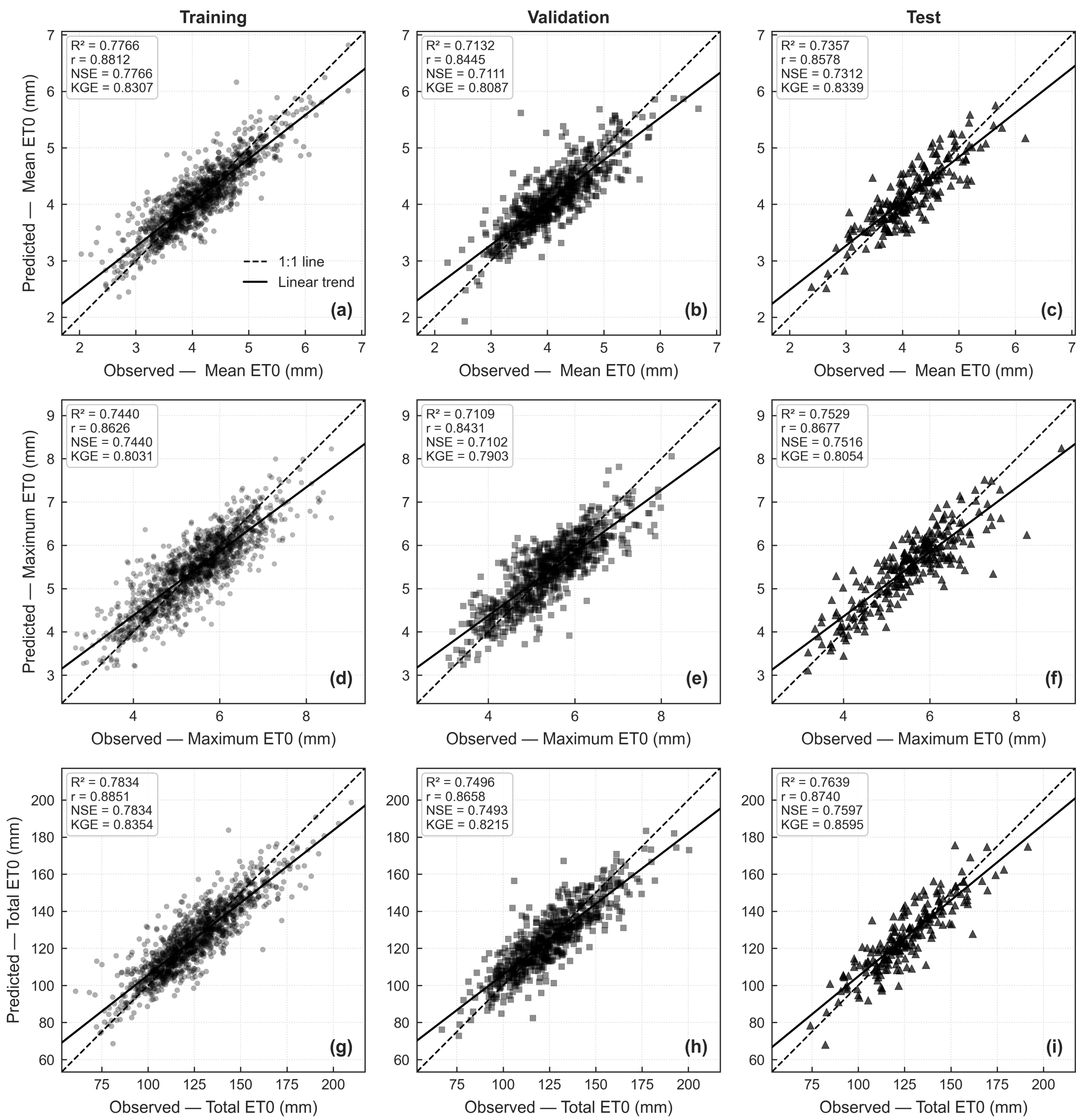

Figure 4. Scatter plots and Pearson correlation of observed and estimated $\overline{\mathrm{ET}}_0$, $\overline{\mathrm{ET}}_{0\text{ - Max}}$ and $\overline{\mathrm{ET}}_{0\text{ - Total}}$ values with the ANN models, using ERA5 reanalysis data and top-of-atmosphere radiation as inputs.

Figures 5, 6, and 7 present the spatial and temporal distribution maps of $\overline{\mathrm{ET}}_0$, $\overline{\mathrm{ET}}_{0\text{ - Max}}$ and $\overline{\mathrm{ET}}_{0\text{ - Total}}$ for the State of Mato Grosso, highlighting the Amazon, Brazilian Savannah, and Pantanal biomes. Figure 8 shows the average monthly values of these variables in the three biomes.

The maps in Figures 5-7, along with the average values presented in Figure 8, show that the Pantanal exhibits the highest ET_0 demand during the months from October to March, corresponding to spring and summer. The Amazon and the Brazilian Savannah come next, with less demand. During the mentioned period, the average values of $\overline{\mathrm{ET}}_0$, $\overline{\mathrm{ET}}_{0\text{ - Max}}$ and $\overline{\mathrm{ET}}_{0\text{ - Total}}$ for the Pantanal range between 4.4 and 5.1 mm day^{-1}, 6.1 and 6.9 mm day^{-1}, and between 129.2 and 158.1 mm month^{-1}, respectively. For the Brazilian Savannah and the Amazon, these values range between 3.7 and 4.8 mm day^{-1}, 5.2 and 6.4 mm day^{-1}, and between 108.3 and 147.6 mm month^{-1}, respectively.

However, from May to August (autumn and winter), this behavior is reversed. During this period, the Pantanal presented the lowest ET_0 demand, whereas the Brazilian Savannah and Amazon recorded the highest values. For these two biomes, ET_0 during this period had similar values for $\overline{\mathrm{ET}}_0$ and $\overline{\mathrm{ET}}_{0\text{ - Total}}$, but higher values still occurred in the Brazilian savanna areas. The averages of $\overline{\mathrm{ET}}_0$, $\overline{\mathrm{ET}}_{0\text{ - Max}}$ and $\overline{\mathrm{ET}}_{0\text{ - Total}}$ for the Brazilian Savannah and the Amazon during this period range between 3.4 and 4.6 mm day^{-1}, 4.2 and 5.9 mm day^{-1}, and between 103.7 and 139.8 mm month^{-1}, respectively. For the Pantanal, these values range between 2.6 and 3.7 mm day^{-1}, 3.7 and 5.1 mm day^{-1}, and between 87.7 and 118.3 mm month^{-1}, respectively. The quarter with the highest ET_0 demand in the Brazilian Savannah and Amazon occurred in August, September, and October, representing the end of winter and the beginning of spring. The highest values of $\overline{\mathrm{ET}}_0$ and $\overline{\mathrm{ET}}_{0\text{ - Total}}$ were observed in the last two months. During this period, both the Brazilian Savannah and the Amazon record variations between 4.2 and 4.8 mm day^{-1} for $\overline{\mathrm{ET}}_0$, 5.5 and 6.4 mm day^{-1} for $\overline{\mathrm{ET}}_{0\text{ - Max}}$, and between 130.6 and 147.6 mm month^{-1} for $\overline{\mathrm{ET}}_{0\text{ - Total}}$.

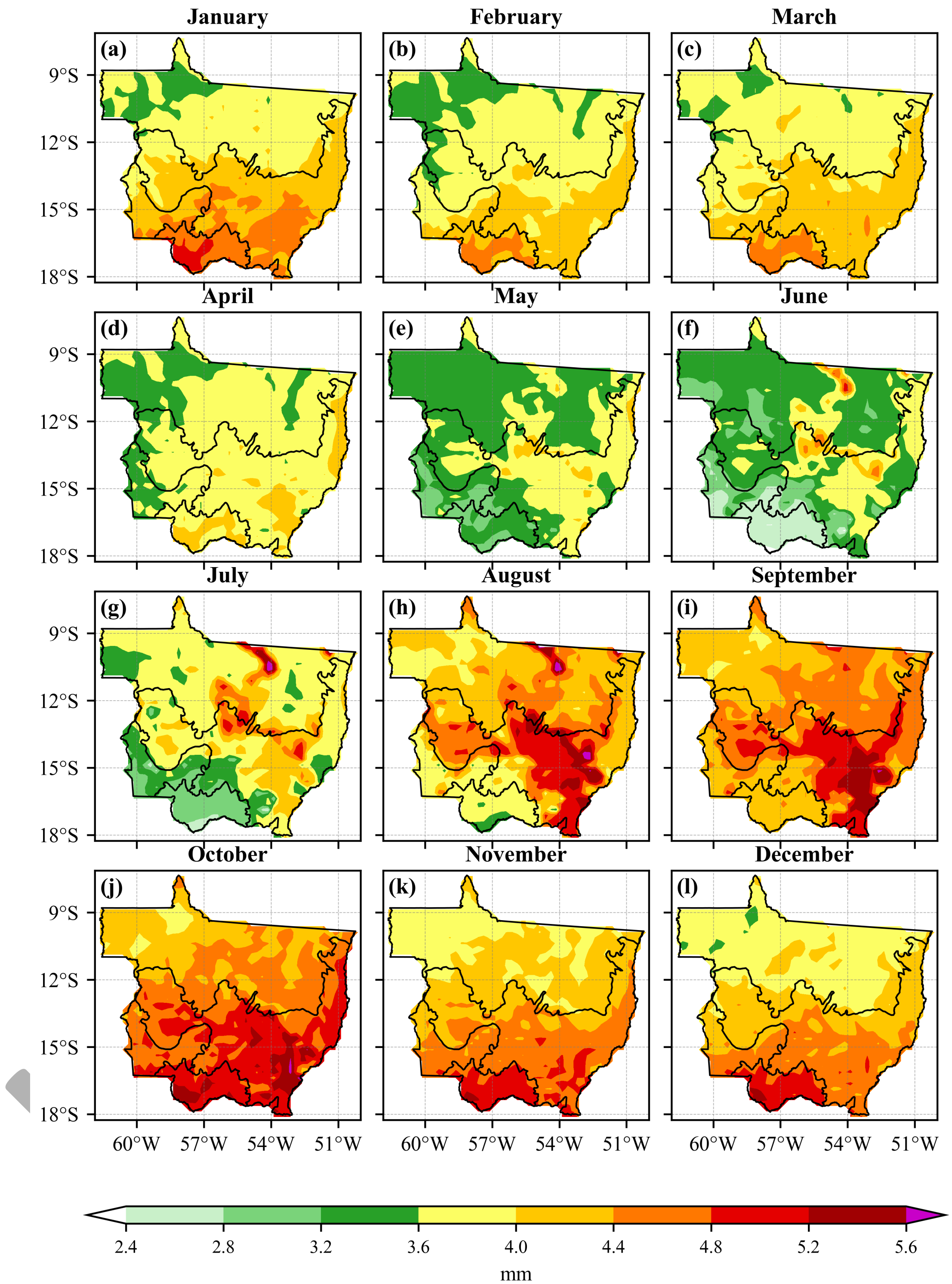

Figure 5. Spatial distribution of average daily monthly reference evapotranspiration (mm day^{-1}) for the period from 1980 to 2019 in the State of Mato Grosso, obtained with the ANN model.

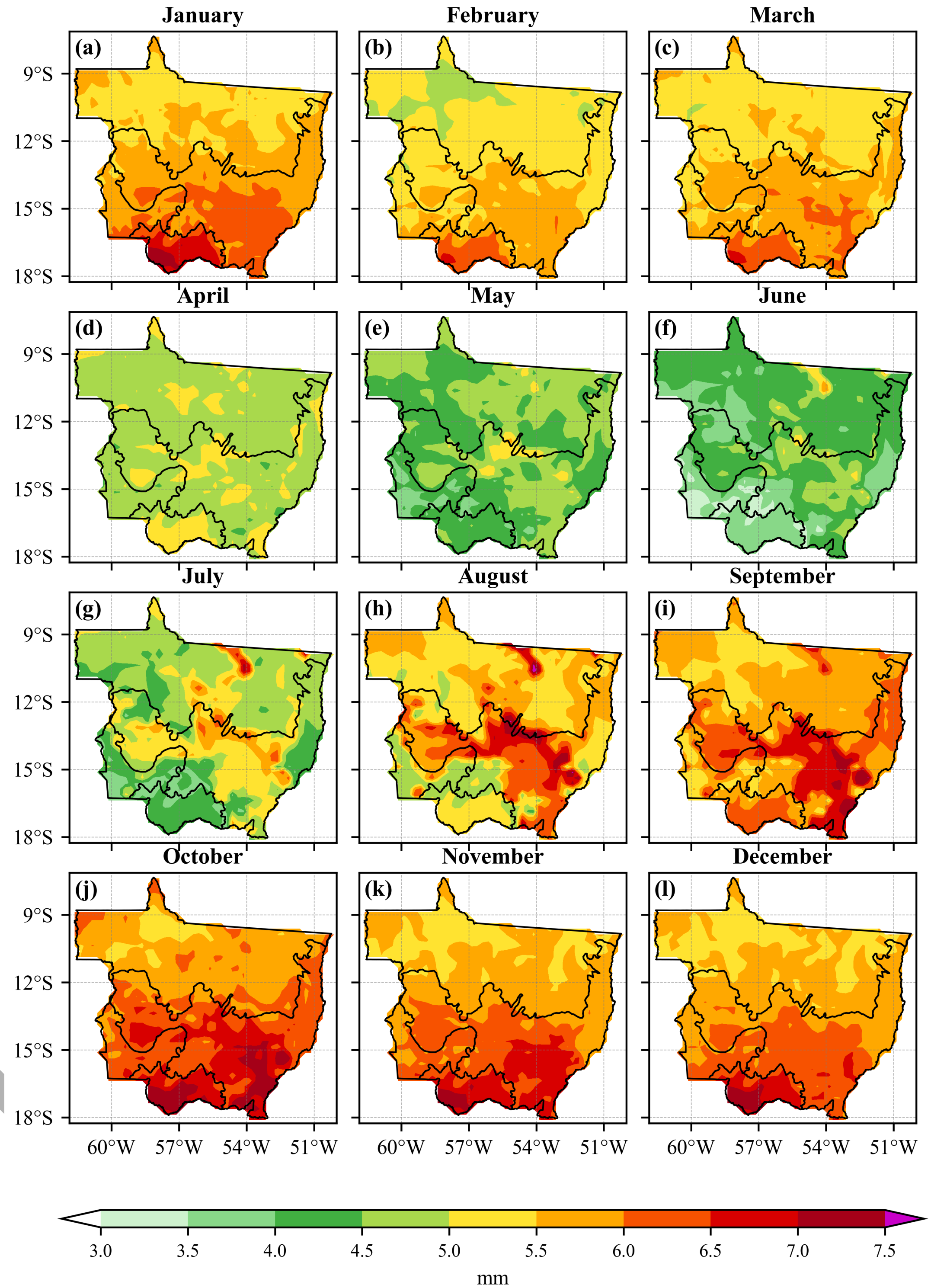

Figure 6. Spatial distribution of maximum daily monthly reference evapotranspiration (mm day^{-1}) for the period from 1980 to 2019 in the State of Mato Grosso, obtained with the ANN model.

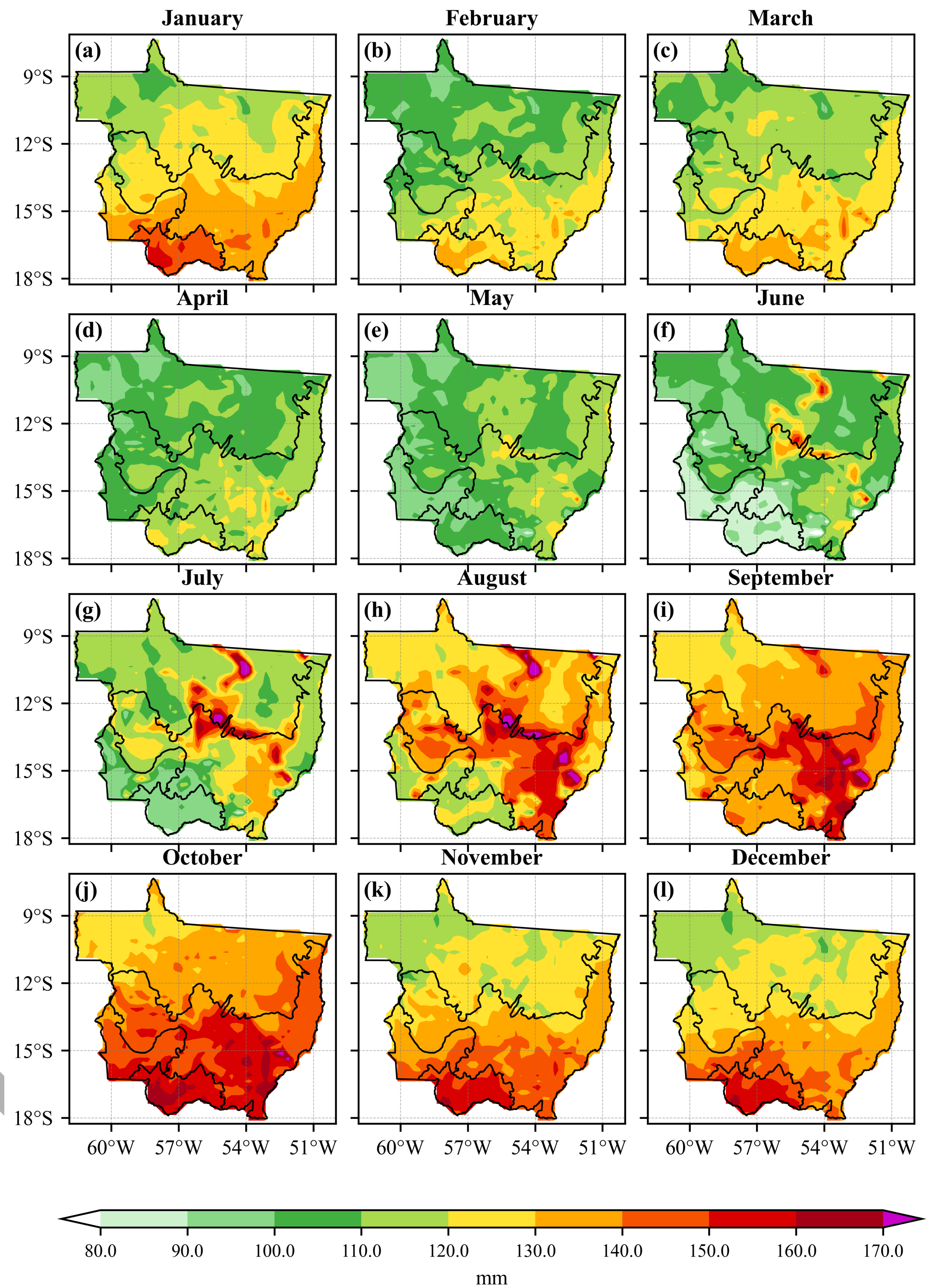

Figure 7. Spatial distribution of total monthly reference evapotranspiration (mm month^{-1}) for the period from 1980 to 2019 in the State of Mato Grosso, obtained with the ANN model.

Figure 8 shows that October had the highest $\overline{ET}_{0\text{ - Max}}$ values, ranging from 5.9 to 6.9 mm day^{-1}. In the Pantanal, October (spring) is the month with the highest average daily, maximum daily monthly and total monthly ET_0 demand, with values of 5.1 mm day^{-1}, 6.9 mm day^{-1} and 158.1 mm month^{-1}, respectively.

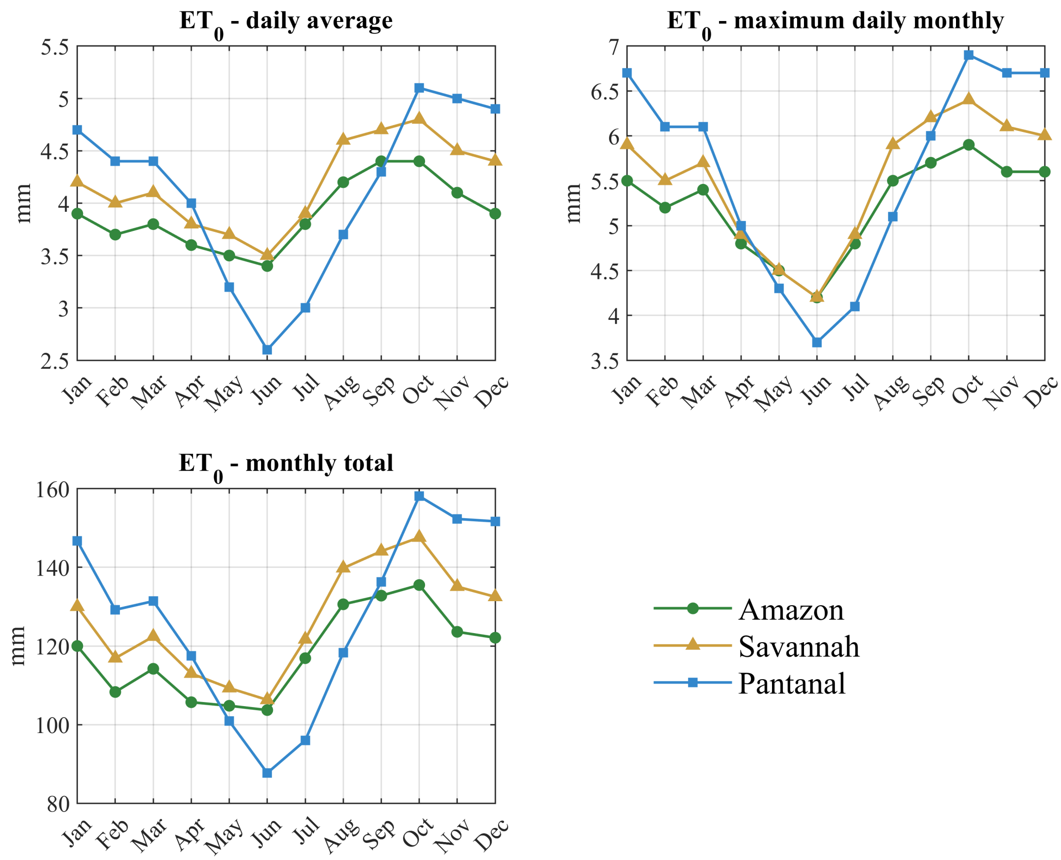

Figure 8. Average daily monthly reference evapotranspiration, maximum daily monthly evapotranspiration, and total monthly evapotranspiration for the period from 1980 to 2019, estimated with the Artificial Neural Network models for the biomes of the State of Mato Grosso.

The lowest ET_0 values occurred from April to June, corresponding to autumn and the beginning of winter. In the Pantanal, the lowest ET_0 demand occurs in June, with values of 2.6 mm day^{-1} for $\overline{ET}_0$, 3.7 mm day^{-1} for $\overline{ET}_{0\text{ - Max}}$, and 87.7 mm month^{-1} for $\overline{ET}_{0\text{ - Total}}$. In the Brazilian Savannah and Amazon of Mato Grosso, May and June have the lowest evapotranspiration demands, with values ranging between 3.4 and 3.7 mm day^{-1} for $\overline{ET}_0$, 4.2 and 4.5 mm day^{-1} for $\overline{ET}_{0\text{ - Max}}$, and 103.7 and 109.3 mm month^{-1} for $\overline{ET}_{0\text{ - Total}}$.

Figure 9 presents the $\overline{ET}_0$, $\overline{ET}_{0\text{ - Max}}$ and $\overline{ET}_{0\text{ - Total}}$ values for the capital and main grain-producing cities in Mato Grosso.

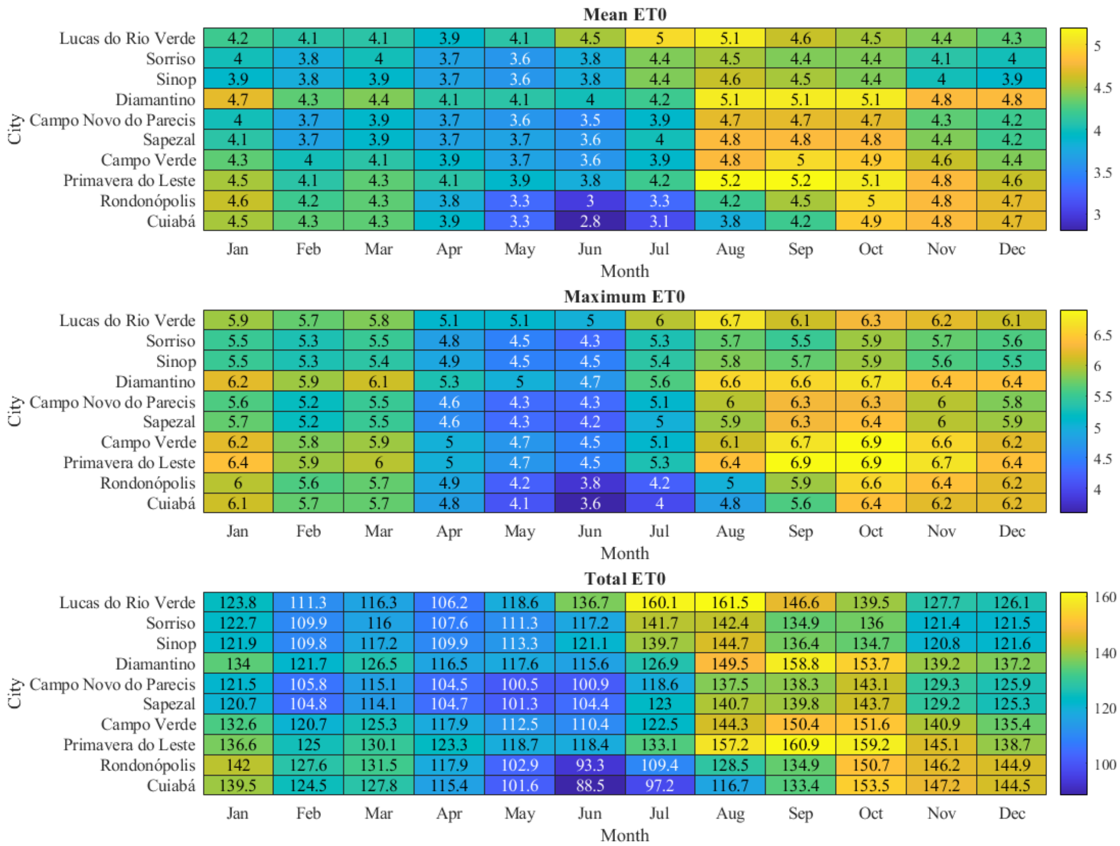

Figure 9. Monthly mean daily reference evapotranspiration ($\overline{ET}_0$, mm day^{-1}), monthly maximum daily reference evapotranspiration ($\overline{ET}_{0\text{ - Max}}$, mm day^{-1}), and total monthly reference evapotranspiration ($\overline{ET}_{0\text{ - Total}}$, mm month^{-1}) from 1980 to 2019 for the state capital and principal grain-producing municipalities in Mato Grosso, Brazil.

The data in Figure 9 more clearly show that the highest reference evapotranspiration demands occurred in August, September, and October, while the lowest occurred between April and June, supporting the results obtained by biomes. Notably, regarding the monthly average daily and monthly maximum daily values, there were no significant differences in the reference evapotranspiration values among the various cities that stood out in grain production.

Figure 10 shows the results of the trend test for the average daily monthly evapotranspiration ($\overline{ET}_0$) from January 1980 to December 2019, performed using the Mann-Kendall test at a 5% significance level. The areas highlighted in red indicate positive trends in evapotranspiration. Examining the map, it was evident that all three biomes showed areas with an increasing trend in $ET_{0.}$

The magnitude of the temporal trends identified by the Mann–Kendall test was quantified using the Sen's slope estimator (Theil-Sen method), as depicted in Figure 11. This figure displays the rates of change in the monthly mean daily reference evapotranspiration ($\overline{ET}_0$), expressed in mm day^{-1} decade^{-1}. The Amazon, Cerrado (Brazilian Savanna), and Pantanal biomes exhibited upward $\overline{ET}_0$ trends, with mean rates of 0.063, 0.061, and 0.090 mm day^{-1} decade^{-1}, respectively.

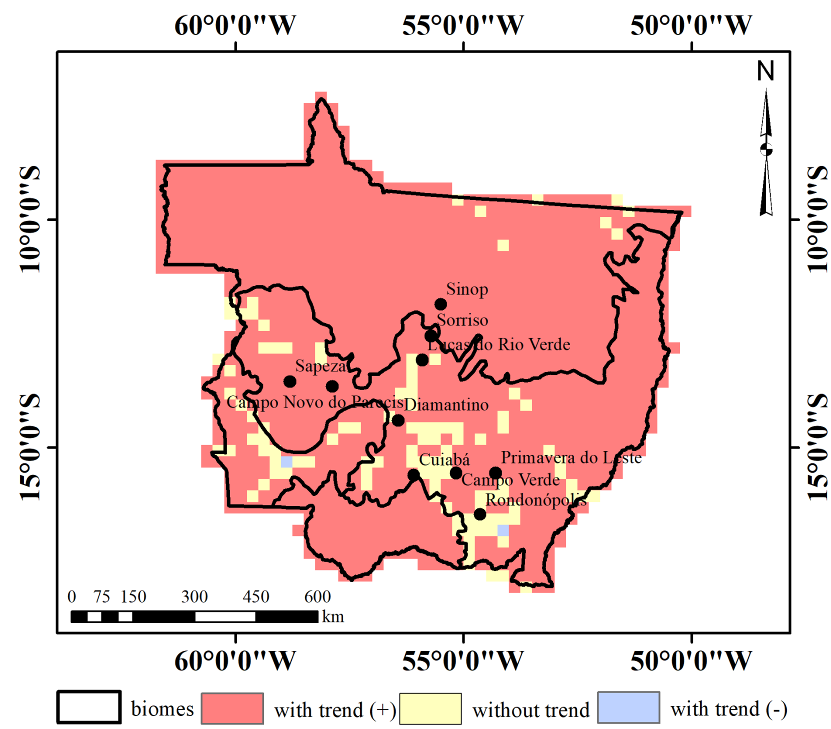

Figure 10. Trend analysis of average daily monthly reference evapotranspiration ($\overline{ET}_0$) in the State of Mato Grosso for the period from 1980 to 2019, using the Mann-Kendall test at a 5% significance level.

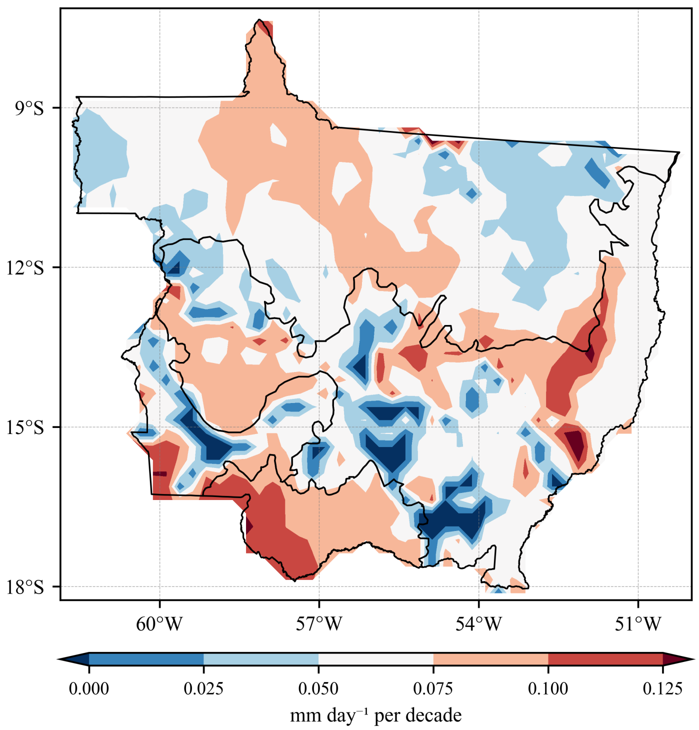

Figure 11. Rate of change in mean daily reference evapotranspiration ($\overline{ET}_0$), estimated using the Sen's slope estimator (Theil-Sen method), expressed in mm day^{-1} decade^{-1}.

4. Discussion

The integration of ERA5 reanalysis data and solar radiation as predictor variables in artificial neural networks facilitated the spatial estimation of reference evapotranspiration (ET_0) across the study area. Model performance metrics consistently demonstrated robust agreement with ET_0 values calculated via the FAO-56 Penman-Monteith equation. This approach is particularly advantageous for regions characterized by low meteorological station density. Spatiotemporal analyses identified pronounced seasonality in evapotranspiration demand, which is critical for quantifying climatic variability and assessing impacts on agricultural productivity and water resources management. Additionally, the identification of statistically significant upward trends in evapotranspiration for biomes such as the Amazon, Pantanal, and Cerrado provides pivotal insights for the development of sustainable land and water management strategies in Brazil. These results underscore the necessity of integrating these trends into the formulation of policy frameworks for natural resource governance and climate change adaptation.

Biudes *et al.* (2022) conducted a study to characterize the temporal and spatial dynamics of evapotranspiration (ET) in Mato Grosso utilizing remote sensing datasets. Employing data collected from eight eddy covariance flux towers and applying the Bowen ratio energy balance method for ET estimation, the researchers validated the MOD16A2 evapotranspiration product throughout the study period. Although the authors' ET estimates, aggregated over eight-day intervals and spanning 2001 to 2020, only partially converge with the findings of our investigation, both studies reveal consistent patterns. The Pantanal biome exhibited the highest ET rates from October to March, while the Cerrado and Amazon biomes recorded comparatively lower values. This concordance underscores the significance of seasonal variability and biome-specific influences on surface energy balance and regional climatic regimes, thereby advancing the understanding of spatiotemporal evapotranspiration variability across diverse Brazilian landscapes.

In the referenced study, the authors employed eddy covariance flux towers to estimate evapotranspiration (ET) using the atmospheric profile method, specifically the Bowen ratio energy balance technique. Given that the State of Mato Grosso encompasses approximately 903,000 square kilometers, equating to one flux tower per 112,800 km², the limited spatial representativeness and scalability of this approach across the entire state is evident, as noted in the Introduction. Establishing the models proposed in the present study with data from only eight sites would be impractical, thereby reinforcing the suitability of the FAO-56 Penman–Monteith equation as the preferred method. Consequently, for technical applications related to water resources planning and management in agricultural and river basin contexts, both the ET_0 estimation methodology advanced in this work and the remote sensing-based approach proposed by Biudes *et al*. (2022) are viable operational alternatives.

A comparative analysis of seasonal meteorological variables by biome, as measured at automatic weather stations (Figure 3), combined with the spatiotemporal distribution of reference evapotranspiration (ET_0) presented in Figures 5 through 8, reveals a qualitative association between climatic conditions and ET_0 patterns. This relationship is especially pronounced for solar radiation, air temperature, and atmospheric humidity. Sabino and Souza (2023) performed a global sensitivity analysis of the FAO-56 Penman–Monteith equation using the Sobol method and identified incident solar radiation as the principal climatic factor driving ET_0 variability in Mato Grosso. Their results further indicate that solar radiation, relative humidity, and wind speed are the primary contributors to ET_0 variability in the study region. Previous studies, such as those by Souza *et al*. (2015, 2016) and Valle Júnior *et al*. (2021), emphasized the need for an accurate estimate or measurement of global radiation to determine ET_0 in Mato Grosso. Both studies highlight that accurate evapotranspiration estimation requires the proper determination of global radiation. The sensitivity analysis conducted by Sabino and Souza (2023) guided the selection of predictor variables for the development of artificial neural network (ANN) models. The eight variables chosen as ANN inputs in this study (maximum, minimum, mean, and dew point temperatures, surface pressure, wind speed, top-of-atmosphere radiation, and global solar radiation) were critical for capturing both spatial and seasonal variations in ET_0 across the diverse regions of Mato Grosso.

In contrast to the ET_0 data obtained in this study (Figure 8) and results from authors such as Souza *et al*. (2015, 2016), a general consistency in ET_0 values estimated by ANN models was observed. A comparison of the monthly daily averages in Figure 8 for the municipality of Sinop with the averages obtained by Souza *et al*. (2015) shows that the percentage differences ranged from approximately 3% to 20%. The percentage differences exceeded 10% in June, July, August, and December. From June to August, the model in this study presented higher values, with the difference ranging between 0.6 and 0.7 mm. In December, the proposed model underestimated ET_0 with values of 3.9 and 4.8 found in this study and by the authors, respectively.

Our results demonstrate the feasibility of satisfactorily estimating ET_0 through artificial intelligence methods using reanalysis meteorological data, which are easily determinable inputs. The data estimated in this study will serve as a basis for planning irrigation projects in regions of Mato Grosso that lack meteorological monitoring, representing fundamental information for investigations of water balance in river basins. The extensive temporal series of ET_0, covering 1980-2019, will allow the assessment of the impact of changes in vegetation cover in different biomes on water loss through evapotranspiration and their influence on other hydrological elements. This analysis extends the reach of earlier research that already took into account anthropogenic changes in the state's land cover during evapotranspiration, such as studies by Lathuillière, Johnson, and Donner (2012) and Dias *et al*. (2015), carried out in Mato Grosso for the years 2000–2009 and 2007–2010, respectively.

The acquired dataset offers an opportunity to compare evapotranspiration levels in the 1980s, when Mato Grosso had vast expanses of native forests, with current data after these areas were converted into agricultural land. This comparison allows for a detailed analysis of changes in evapotranspiration patterns over time, revealing the effects of landscape transformations on hydrological processes. Preliminary results indicated an increasing trend in ET_0 across all biomes of Mato Grosso (Figures 10 and 11), highlighting the need for further studies to identify and quantify the climatic and environmental factors responsible for this pattern.

5. Conclusions

It is possible to accurately and precisely estimate and spatialize reference evapotranspiration (ET_0) using the ERA5 reanalysis grid and artificial neural network models. The proposed methodology enables ET_0 estimation in locations with limited meteorological monitoring, supporting hydrological studies, water resources management, and irrigation projects.

The Pantanal biome had the highest ET_0 values from October to March, followed by the Brazilian savanna and Amazon regions. Throughout Mato Grosso, the months with the highest ET_0 demand are August, September, and October, while April, May, and June have the lowest demand.

From 1980 to 2019, there was an increasing ET_0 trend in all of the biomes in the State of Mato Grosso. The Amazon, Cerrado (Brazilian Savanna), and Pantanal biomes exhibited upward $\overline{ET_0}$ trends, with mean rates of 0.063, 0.061, and 0.090 mm day⁻¹ decade⁻¹, respectively. Future studies should be conducted to investigate the causes of this increasing ET_0 trend.

Conflict of Interest

The authors declare that they have no known competing financial interests or personal relationships that could have appeared to influence the work reported in this paper.

Acknowledgments

The authors acknowledge the Federal University of Mato Grosso and the Institute of Agricultural and Environmental Sciences for their support of this research.

References

Abrishami, N., Sepaskhah, A. R., Shahrokhnia, M. H. (2019). Estimating wheat and maize daily evapotranspiration using artificial neural network. *Theoretical and Applied Climatology*, 135(3-4), 945-958. https://doi.org/10.1007/s00704-018-2418-4

Allen, R. G., Pereira, L. S., Raes, D., Smith, M. (1998). *Crop evapotranspiration*: guidelines for computing crop water requirements (Irrigation and Drainage Paper, 56), FAO, Rome, pp. 300

ANA. (2020). Agência Nacional de Águas. Polos Nacionais de Irrigação: Mapeamento de Áreas Irrigadas com Imagens de Satélite. Brasília. https://cdn.agenciapeixevivo.org.br/media/2020/03/polos-nacionais-irriga%C3%A7%C3%A3o.pdf. Accessed January de 2023.

ANA. (2019). Agência Nacional de Águas. Levantamento da agricultura irrigada por pivôs centrais no Brasil. Brasília. https://www.embrapa.br/busca-de-publicacoes/-/publicacao/1121226/levantamento-da-agricultura-irrigada-por-pivos-centrais-no-brasil. Accessed November de 2023.

Asadi, S., Shahrabi, J., Abbaszadeh, P., and Tabanmehr, S. A. (2013). A new hybrid artificial neural networks for rainfall-runoff process modeling. *Neurocomputing*, 121(2013), 470-480. https://doi.org/10.1016/j.neucom.2013.05.023

Barros, V.R., Souza, A.P., Fonseca, D.C., Silva, L.B.D. (2009). Avaliação da evapotranspiração de referência na Região de Seropédica, Rio de Janeiro, utilizando lisímetro de pesagem e modelos matemáticos. Revista Brasileira de Ciências Agrárias, 4(2), 198-203. https://doi.org/10.5039/agraria.v4i2a13

Biudes, M. S., Geli, H. M., Vourlitis, G. L., Machado, N. G., Pavão, V. M., dos Santos, L. O. F., Querino, C. A. S. (2022). Evapotranspiration seasonality over tropical ecosystems in Mato Grosso, Brazil. *Remote Sensing*, *14*(10), 2482. https://doi.org/10.3390/rs14102482

Carvalho, M. Â. C. C. D., Uliana, E. M., Silva, D. D. D., Aires, U. R. V., Martins, C. A. D. S., Sousa Junior, M. F. , Cruz, I. F., Mendes, M. A. D. S. A. (2020). Drought monitoring based on remote sensing in a grain-producing region in the cerrado–amazon transition, Brazil. *Water*, *12*(12), 3366. https://doi.org/10.3390/w12123366

Copernicus Climate Change Service, (2017). ERA5: Fifth generation of ECMWF atmospheric reanalyses of the global climate. Copernicus Climate Change Service Climate Data Store (CDS), (date of access). Available at: <https://cds.climate.copernicus.eu/cdsapp#!/home>. Access on january 2023.

Dai, L., Fu, R., Zhao, Z., Guo, X., Du, Y., Hu, Z., Cao, G. (2022). Comparison of Fourteen Reference Evapotranspiration Models With Lysimeter Measurements at a Site in the Humid Alpine Meadow, Northeastern Qinghai-Tibetan Plateau. *Frontiers in Plant Science*, 13. https://doi.org/10.3389/fpls.2022.854196

Dias, L. C. P., Macedo, M. N., Costa, M. H., Coe, M. T., Neill, C. (2015). Effects of land cover change on evapotranspiration and streamflow of small catchments in the Upper Xingu River Basin, Central Brazil. *Journal of Hydrology: Regional Studies*, *4*, 108-122. https://doi.org/10.1016/j.ejrh.2015.05.010

Duan, Q., Sorooshian, S., Gupta, V. K. (1992). Effective and efficient global optimization for conceptual rainfall-runoff models. *Water Resour. Res*. 28(4), 1015-1031. https://doi.org/10.1029/91WR02985

Elbeltagi, A., Nagy, A., Mohammed, S., Pande, C. B., Kumar, M., Bhat, S. A., Zsembeli, J., Huzsvai, L., Tamás, J., Kovács, E., Harsányi, E., Juhász, C. (2022). Combination of Limited Meteorological Data for Predicting Reference Crop Evapotranspiration Using Artificial Neural Network Method. *Agronomy*, 12(2), 516. https://doi.org/10.3390/agronomy12020516

Gocić, M., Arab Amiri, M. (2021). Reference Evapotranspiration Prediction Using Neural Networks and Optimum Time Lags. *Water Resources Management*, 35(6), 1913-1926. https://doi.org/10.1007/s11269-021-02820-8

Gorelick, N., Hancher, M., Dixon, M., Ilyushchenko, S., Thau, D., Moore, R. (2017). Google Earth Engine: Planetary-scale geospatial analysis for everyone. *Remote Sensing of Environm*ent, 202, 18-27. https://doi.org/10.1016/j.rse.2017.06.031

Guo D., Westra S., Peterson T. (2022). Evapotranspiration: Modelling Actual, Potential and Reference Crop Evapotranspiration_. R package version 1.16. Available at: <https://CRAN.R-project.org/package=Evapotranspiration>. Access on january 2023.

Guo, D., Westra, S., Maier, H. R. (2016). An R package for modelling actual, potential and reference evapotranspiration. *Environmental Modelling & Software* 78, 216-224. https://doi.org/10.1016/j.envsoft.2015.12.019

Hersbach, H., Bell, B., Berrisford, P. *et al*. (2020). The ERA5 global reanalysis. *Quarterly Journal of the Royal Meteorological Society* 146(730), 1999-2049. https://doi.org/10.1002/qj.3803

IBGE (2017). Instituto Brasileiro de Geografia e Estatística. Censo Agropecuário 2017. Rio de Janeiro. https://censoagro2017.ibge.gov.br/. Accessed 14 November 2023.

Kling, H., Fuchs, M., & Paulin, M. (2012). Runoff conditions in the upper Danube basin under an ensemble of climate change scenarios. *Journal of Hydrology, 424–425*, 264–277. https://doi.org/10.1016/j.jhydrol.2012.01.011

Laqui, W., Zubieta, R., Rau, P., Mejía, A., Lavado, W., Ingol, E. (2019). Can artificial neural networks estimate potential evapotranspiration in Peruvian highlands? *Modeling Earth Systems and Environment*, 5(4), 1911-1924. https://doi.org/10.1007/s40808-019-00647-2

Lathuillière, M. J., Johnson, M. S., Donner, S. D. (2012). Water use by terrestrial ecosystems: temporal variability in rainforest and agricultural contributions to evapotranspiration in Mato Grosso, Brazil. *Environmental Research Letters*, *7*(2), 024024. https://doi.org/10.1088/1748-9326/7/2/024024

Liu, X., XU, C., Zhong, X., Li, Y.; Yuan, X.; Cao, J. (2017). Comparison of 16 models for reference crop evapotranspiration against weighing lysimeter measurement. *Agricultural Water Management*, 184, 145-155. https://doi.org/10.1016/j.agwat.2017.01.017

Liu, G., Liu, Y., Hafeez, M., Xu, D., Vote, C. (2012). Comparison of two methods to derive time series of actual evapotranspiration using eddy covariance measurements in the southeastern Australia. Journal of Hydrology. 454–455, 1–6. https://doi.org/10.1016/j.jhydrol.2012.05.011

Morgan Uliana, E., de Abreu Araujo, J., Roggia Zanuzo, M., Guedes Araujo, A. H., Fomaca de Sousa Junior, M., Venâncio Aires, U. R., & Alves Ramos Filho, H. (2025). Estimation of Global Solar Radiation in Unmonitored Areas of Brazil Using ERA5 Reanalysis and Artificial Neural Networks. *Atmosphere*, *16*(11), 1306.

Nouri, M.; Homaee, M. (2022). Reference crop evapotranspiration for data-sparse regions using reanalysis products. *Agricultural Water Management*, 262, 107319. https://doi.org/10.1016/j.agwat.2021.107319

Pereira, A. R., Sediyama, G. C., Villa Nova, N. A. (2013). *Evapotranspiração*, Fundag, Campinas, pp. 323.

R Core Team (2022). R: A language and environment for statistical computing. R Foundation for Statistical Computing, Vienna, Austria. Available at: <https://www.R-project.org/>. Access on january 2023.

Ramos Filho, H. A.., Uliana, E. M., Aires, U. R. V., da Cruz, I. F., Lisboa, L., da Silva, D. D., Viola, M.R., Duarte, V. B. R. (2024). Nowcast flood predictions in the Amazon watershed based on the remotely sensed rainfall product PDIRnow and artificial neural networks. *Environmental Monitoring and Assessment*, *196*(3), 245. https://doi.org/10.1007/s10661-024-12396-6

Rodrigues, G. C., Braga, R. P. (2021). Estimation of Daily Reference Evapotranspiration from NASA POWER Reanalysis Products in a Hot Summer Mediterranean Climate. *Agronomy*, 11(10), 2077. https://doi.org/10.3390/agronomy11102077

Sabino, M., Souza, A. P. (2023). Global Sensitivity of Penman–Monteith Reference Evapotranspiration to Climatic Variables in Mato Grosso, Brazil. *Earth*, *4*(3), 714-727. https://doi.org/10.3390/earth4030038

Saha, A., Boughton, E. H., Li, H., Sonniér, G., Gomez-Casanovas, N., Mcmillan, N., Zhang, X. (2022). Evapotranspiration in a subtropical wetland savanna using low-cost lysimeter, eddy covariance and modelling approaches. *Ecohydrology*, 15(8). https://doi.org/10.1002/eco.2475

Santiago, A.V., Pereira, A.R., Folegatti, M.V., Maggiotto, S.R. (2002). Evapotranspiração de referência medida por lisímetro de pesagem e estimada por Penman-Monteith (FAO-56), nas escalas mensal e decendial. Revista Brasileira de Agrometeorologia, 10(1), 57-66.

Silva, E. H. F. M., Hoogenboom, G., Boote, J., Gonçalves, A. O., Marin, F. R. (2022). Predicting soybean evapotranspiration and crop water productivity for a tropical environment using the CSM-CROPGRO-Soybean model. *Agricultural and Forest Meteorology*, 323, 109075. https://doi.org/10.1016/j.agrformet.2022.109075

Sousa Jr, M. F., Uliana, E. M., Aires, R. V. U., Rápalo, L. M. C., da Silva, D. D., Moreira, M. C., Lisboa, L., da Silva Rondon, D. (2024). Streamflow prediction based on machine learning models and rainfall estimated by remote sensing in the Brazilian Savanna and Amazon biomes transition. *Modeling Earth Systems and Environment*, *10*(1), 1191-1202. https://doi.org/10.1007/s40808-023-01837-9

Souza, A. P., Tanaka, A. A., da Silva, A. C., Uliana, E. M., de Almeida, F. T., Gomes, A. W. A., Klar, A. E. (2016). Reference evapotranspiration by Penman–Monteith FAO 56 with missing data of global radiation. *Revista Brasileira de Engenharia de Biossistemas*, *10*(2), 217-233. https://doi.org/10.18011/bioeng2016v10n2p217-233

Souza, A. P., de Almeida, F. T., Arantes, K. R., Martim, C. C., da Silva, J. O. (2015). Coeficientes de Tanque Classe A para estimativa da evapotranspiração de referência diária na região de transição Cerrado-Amazônica. *Scientia Plena*, *11*(5).

Tari, A. F., Nacar, M. S., Nacar, A. S., Akin, S. (2022). Comparison of some evapotranspiration models using lysimeter measurements in arid climate conditions. *Irrigation and Drainage*, 71(4), 948-958. https://doi.org/10.1002/ird.2707

Tian, Y., Zhang, K., Xu, Y., Gao, X., Wang, J. (2018). Evaluation of Potential Evapotranspiration Based on CMADS Reanalysis Dataset over China. *Water*, 10(9), 1126, 2018. https://doi.org/10.3390/w10091126

Uliana, E. M., Aires, U. R. V., de Sousa Junior, M. F., da Silva, D. D., Moreira, M. C., da Cruz, I. F., Araujo, H. B. (2024). Estimated evaporation of lakes by climate reanalysis data and artificial neural networks. *Journal of South American Earth Sciences*, *136*, 104811. https://doi.org/10.1016/j.jsames.2024.104811

Valle Júnior, L. C. G. D., Vourlitis, G. L., Curado, L. F. A., Palácios, R. D. S., Nogueira, J. D. S., Lobo, F. D. A., Islam, A. R. M. T., Rodrigues, T. R. (2021). Evaluation of FAO-56 procedures for estimating reference evapotranspiration using missing climatic data for a Brazilian tropical savanna. *Water*, *13*(13), 1763. https://doi.org/10.3390/w13131763

Van Liew, M. W., Veith, T. L., Bosch, D. D., and Arnold, J. G. (2007). Suitability of SWAT for the conservation effects assessment project: a comparison on USDA-ARS watersheds. *J. Hydrol. Eng*. 12(2), 173-189. https://doi.org/10.1061/(ASCE)1084-0699(2007)12:2(173)

Walls, S., Binns, A. D., Levison, J.; Macritchie, S. (2020). Prediction of actual evapotranspiration by artificial neural network models using data from a Bowen ratio energy balance station. *Neural Computing and Applications*, 32(17), 14001-14018. https://doi.org/10.1007/s00521-020-04800-2

Woldesenbet, T. A., Elagib, N. A. (2021). Spatial-temporal evaluation of different reference evapotranspiration methods based on the climate forecast system reanalysis data. *Hydrological Processes*, 35(6). https://doi.org/10.1002/hyp.14239

Xiong, Y., Chen, X., Tang, L., Wang, H. (2022). Comparison of surface renewal and Bowen ratio derived evapotranspiration measurements in an arid vineyard. *Journal of Hydrology*, 613, 128474. https://doi.org/10.1016/j.jhydrol.2022.12847

Yan, H., Li, M., Zhang, C., Zhang, J., Wang, G., Yu, J., Ma, J., Zhao, S. (2022). Comparison of evapotranspiration upscaling methods from instantaneous to daytime scale for tea and wheat in southeast China. *Agricultural Water Management*, *264*, 107464. https://doi.org/10.1016/j.agwat.2022.107464